Research of Pattern Formation, edited by R. Takaki, pp. 411–430.

Evolution of Antiphase Ordered Domain Structure and Phase Separation Activated by Ordering

Kenichi SHIIYAMA, Hiroshi NINOMIYA, and Tetsuo EGUCHI

Department of Applied Physics, Fukuoka University, Fukuoka 814-01, Japan

Abstract. Computer simulations in two dimensions were carried out on the dynamics of pattern formations of ordered domain structures on isothermal ageing in ordering alloys, which are observed under an electron microscope as dark field images by the use of superstructure reflections. Three cases were considered: the first case is a simple one of the evolution of antiphase ordered domain structures in an alloy of uniform composition, often observed in various binary alloys. In particular, the results of our simulation were compared satisfactorily with the observed features of formation and movement of antiphase boundaries (APBs) in Fe_3Al on ordering from B2 to DO_3. The second case is the pattern formation of antiphase structures on phase separation induced by ordering, observed in Fe_3Al. In this case both the local degree of order and the local composition variable are coupled to change with ageing time. The pattern obtained by our simulation has an excellent similarity to the ones observed under an electron microscope in Fe_3Al on the phase transition from B2 to A2 + DO_3. The third case is also the phase separation activated by ordering, but with a high anisotropy, as is observed in Fe-Si on the phase transition from B2 to B2 + DO_3. All through our simulation we have used a continuum model for the alloy under consideration, which is represented by the local degree of order and the local composition parameter. The equations of motion for these variables have been derived from an appropriate thermodynamical potential by the method of so-called TDGL (time-dependent Ginzburg-Landau). The overall agreement of our results of simulated patterns and the corresponding observed electron micrographs indicates the adequateness of the TDGL method, and suitableness of our thermodynamical potential.

1. Introduction

Alloys have many countenances. They look differently depending upon which means are used to observe them. By naked eyes, for example, their colors, shininess, shapes etc. are seen. Under optical microscopes, they show us their textures, grain boundaries etc. Or, under high resolution electron microscopes, their patterns of atomic arrangements are observed as their lattice images in nm world. Here in this report, we shall discuss on the countenances of alloys in μm order of magnitude, which are quite different from those in mm or nm world, and furthermore, those countenances or patterns change rapidly at first and then slowly later with ageing time. We are particularly interested in their images when they are observed in an electron microscope as dark field images using a superstructure reflection. In this case the ordered regions in the alloy are observed in white contrast, whereas the disordered ones and the antiphase boundaries (APBs) in black one.

Photo. 1 shows examples of electron micrographs of CuZn and FeCo in the ordered state, as dark field images by the use of 100 superstructure reflection, taken by Tomokiyo (1989). In these micrographs of the typical ordering alloys, the antiphase ordered domain structures are recognized. The next example, Photo. 2, is a series of dark field images of Fe_3Al taken with the DO_3 superstructure reflection, by Oki *et al.* (1974, 1977), showing the evolution of ordered DO_3 phases among disordered ones in the course of ordering from B2 to DO_3. By our analysis (Eguchi

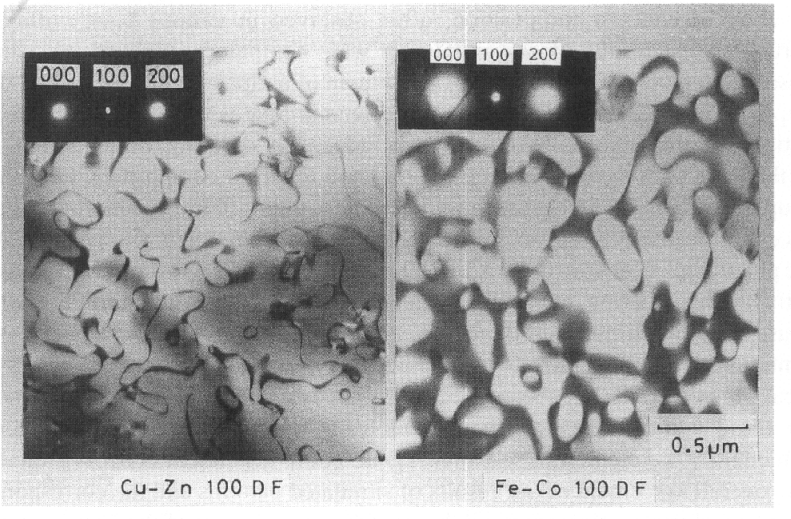

Photo. 1. Dark field images of electron micrographs of ordered CuZn and FeCo taken with the 100 superstructure reflection. White regions show the ordered phases, and the black ones the antiphase boundaries (APBs). Courtesy by Tomokiyo (1989).

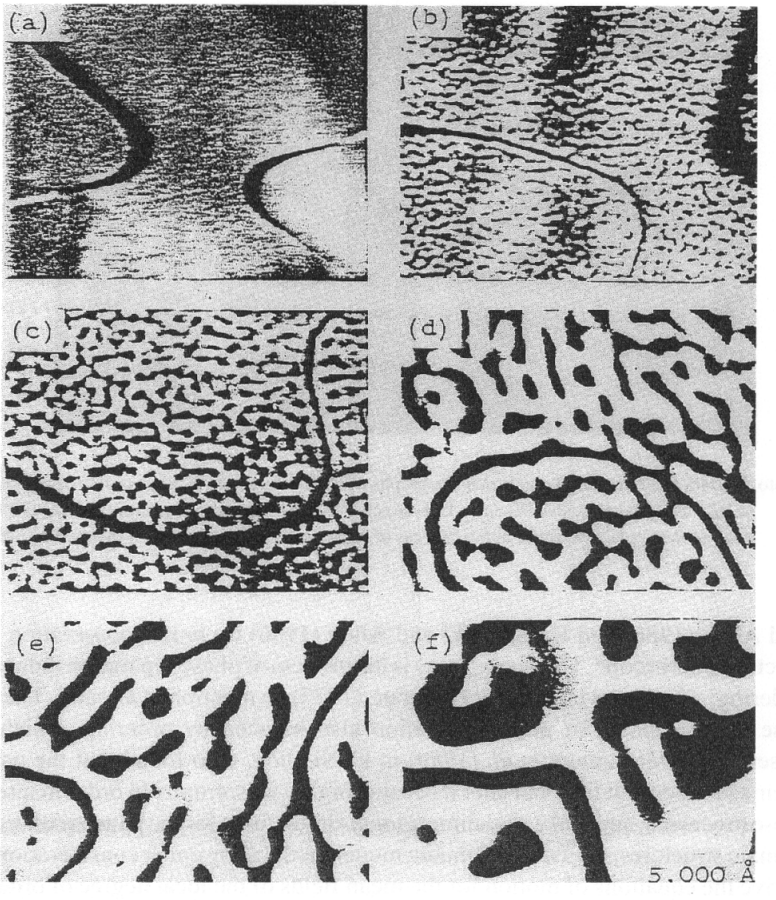

Photo. 2. Dark Field images of electron micrographs of Fe_3Al, showing the process of ordering from B2 to A2(α) + DO_3, taken with a DO_3 superstructure reflection (Oki *et al.*, 1974, 1977). The process is a typical example of the isotropic phase separation induced by ordering.

et al., 1984) it has become clear that these patterns are created by the process of phase separation activated by ordering. The third example, Photo. 3, is a series of electron micrographs of Fe-Si alloy in the course of ordering also from B2 to B2 + DO_3 taken by Matsumura *et al.* (1989), which, however, show highly anisotropic phase separation and ordering.

The main subject of the present report consists of the three parts. The first one is the evolution of antiphase ordered domain structure, like the ones in Photo. 1, on anneal-ageing an alloy from its disordered state. The process has most extensively studied in Fe_3Al by Matsumura (1990) and by Allen and Krzanowski (1985), Park

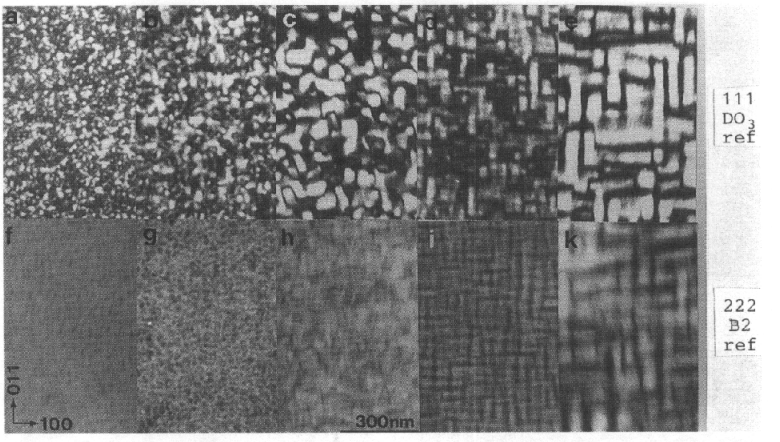

Photo. 3. Dark field images of electron micrographs of Fe-Si, showing the process of ordering from B2 to B2 + DO_3, taken with a B2 and a DO_3 superstructure reflection (Matsumura *et al.*, 1989). The process is a typical example of the process of anisotropic phase separation induced by ordering.

and Allen (1986) and Krzanowski and Allen (1986) by *in situ* observation in an electron microscope. The second case is the process of phase separation induced by ordering, which was studied by Oki *et al.* (1977) as mentioned already. The third case is the process of phase separation also induced by ordering, which was observed by Matsumura *et al.* (1989) in Fe-Si alloy, who found that the process seemed isotropic at first, but later it became highly anisotropic. In order to interpret these processes, and make two-dimensional simulations for the patterns of ordered domain structures, we use a continuum model for the alloy under consideration, and derive the equations of motion for the mean fields of the local degree of order $s(\boldsymbol{r}, t)$ and/or the local compositional variation $x(\boldsymbol{r}, t)$, under suitable assumptions as to the thermodynamical potential of the system, which comprise the bulk free energy and interfacial energy along the interfaces of changing degree of order or compositional field.

2. Process of Formation of Antiphase Ordered Domain Structure

In our first case of an evolution of antiphase ordered domain structure, readers are called for their attention to the experimental result by Matsumura (1989), Photo. 4, who observed the process of DO_3 ordering of Fe_3Al, after quenching from B2 state, in an electron microscope by the dark field image method using the DO_3 superstructure reflection. Here, the small domains of imperfect degree of order are created randomly among disordered (B2) matrix, and they change their shapes and sizes vividly in the early stage of isothermal ageing. As the anneal-ageing proceeds

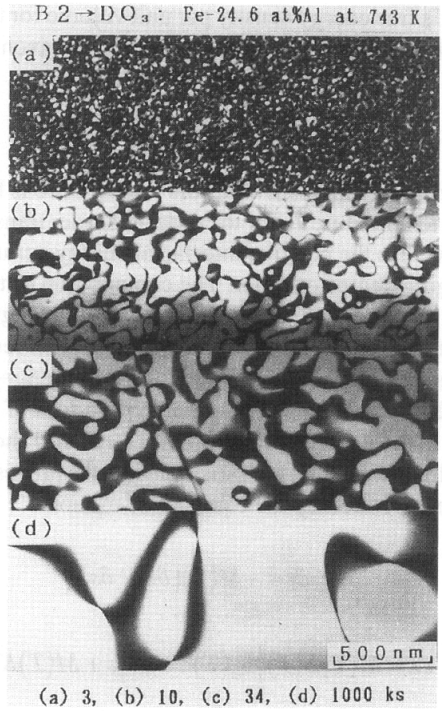

Photo. 4. Dark field images of electron micrographs of Fe_3Al, showing the process of ordering from B2 to DO_3, taken with a DO_3 superstructure reflection (Matsumura, 1990).

those domains grow larger and sometimes they begin to coalesce when two of them, which happen to be of the same phase, become in contact. On further annealing the ordered domains grow in their sizes and the degrees of order. After the disordered phase disappeared, only the ordered domains and APBs remain to exist. The *in situ* observation by Park and Allen (1986) in this later stage of ageing shows that the APBs move slowly to smooth themselves, and small domains keep shrinking and then disappear.

In order to analyze such a process of evolution of antiphase ordered domain structure, we start from the thermodynamical potential of the following form, which includes only the local degree of order $s(\boldsymbol{r}, t)$ as a continuous field variable (Ninomiya *et al.*, 1990).

$$F\left[\{s(\boldsymbol{r},t)\}\right] = \int \left\{ f(s) + \left(K(T)/2\right)(\nabla s)^2 \right\} d^3r \qquad (1)$$

where $f(s)$ is Landau's free energy density per unit volume for the system undergoing the order-disorder transition of the second order, as given by

$$f(s) = -A(T)s^2 / 2 + B(T)s^4 / 4. \tag{2}$$

$A(T)$ changes from negative to positive, as the temperature is lowered from above to below the critical temperature T_0 for the order-disorder transition, whereas $B(T)$ is always positive. $K(T)$ is the positive interfacial energy per unit length along the boundaries of changing degree of order. The composition of the alloy is assumed constant uniformly in the alloy. Now the equilibrium degree of order at the temperature T is obtained from (2) by minimizing $f(s)$ with respect to s, or $df/ds = 0$, as $s = \pm S_e(T)$, where $S_e(T) = \{A(T)/B(T)\}^{1/2}$ for $T < T_0$, or $S_e = 0$ when $T > T_0$. This means that the critical temperature T_0 is given by the root of $A(T) = 0$. The equilibrium distribution of the local degree of order $s(r, t) = s(r)$ should be given by $\delta F/\delta s = 0$, If, however, this condition is not satisfied, then the process of relaxation takes place, which will be described by the equation of motion:

$$\partial s / \partial t = -M(T)(\delta F / \delta s),$$

$$\text{or} \quad \partial s / \partial t = M(T)B(T)\left\{S_e(T)^2 - s^2\right\}s + M(T)K(T)\nabla^2 s, \tag{3}$$

where $M(T)$ is the positive reaction rate depending upon the temperature T. After certain suitable scale changes, the above equation of motion reduces into a simple nonlinear partial differential equation, which is valid for the case of isothermal ageing:

$$\partial s / \partial t = s\left(1 - s^2\right) + \nabla^2 s, \tag{4}$$

in a new dimensionless space-time world.

In the actual calculation Eq. (4) was replaced by a corresponding difference equation, which was solved at first in a one-dimensional mesh of 640 points, and then in a two-dimensional mesh of 200×200 points. The periodic conditions at the boundaries were imposed as usual, and, as the starting values for $s(r, 0)$, a series of small random numbers around zero level were distributed among the mesh, in order to represent the noise of the degree of order introduced in the course of quenching from disordered state at a high temperature to a low one, preceding the ageing at the temperature T below T_0. The integration of Eq. (4) by a small time-interval Δt was repeated, and the number of iteration in our simulation corresponds to the ageing time in the actual experiment.

Figure 1 shows an example for the one-dimensional simulation for the

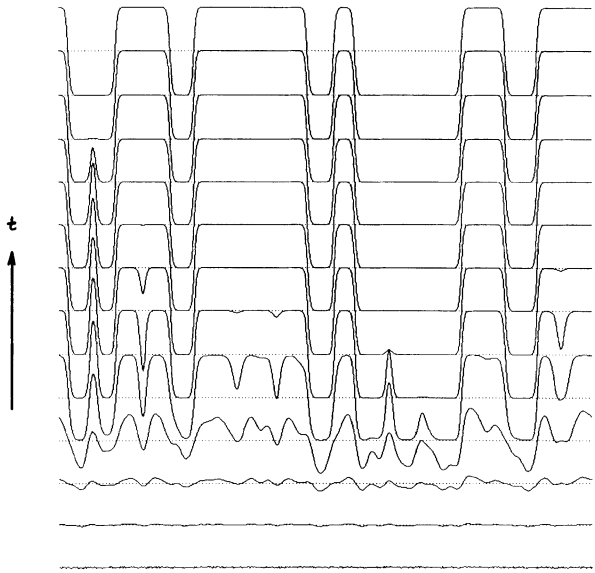

Fig. 1. One-dimensional simulation of the development of antiphase ordered domain structure, based on Eq. (4). The solution started from a series of small random noises at the bottom of the figure, and ended up with a structure of ordered domains structure shown at the top, with the saturated degree of order but with the opposite phases and APBs between them.

evolution of antiphase domain structure, where one can observe that at first an irregular wave with various wavelengths and waveheights is created from the initial noise, but that the wave gradually changes its shape into the domains of various sizes with opposite phases and saturated degree of order. The domain boundary between two fully grown domains with different phases, or of $s = +1$ and $s = -1$, shows a definite magnitude of slope of s, which coinsides with that of the stationary solution of Eq. (4), obtained analytically as $s(r) = \tanh(r/\sqrt{2})$, under the boundary conditions $s = 0$ at $r = 0$ and $ds/dr = 0$ at $r = \pm\infty$. At this stage, the pattern, or the shape of the wave, has almost ceased to change.

Now, look at the two-dimensional simulation shown in Fig. 2. Since we are looking at the pattern of s^2, rather than s itself, in the electron microscopy by the method of dark field images by the use of a superstructure reflection, both the pattern of s, calculated directly from Eq. (4), and the one of s^2 are shown in Fig. 2. In the pattern of s, given in the lower frame, the value of s at each mesh point is represented either in white if $s > 0$ or in black otherwise, whereas in the s^2 pattern, shown in the upper frame, the point is either white if $s^2 > .1$ or black otherwise. As is seen in Fig. 2, a vivid change in the pattern of s takes place in the early stage of ageing, but the magnitude of degree of order is still too small to be recognized as

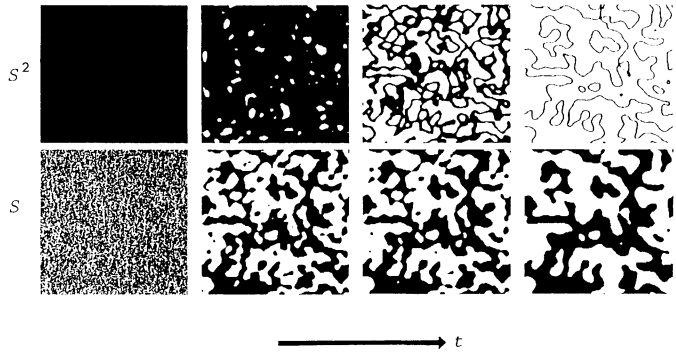

Fig. 2. Two-dimensional simulation of the development of antiphase ordered domain structure, based on Eq. (4). The solution started from a series of small random noises at the left side of the figure, and ended in a structure of ordered domains and APBs shown at the right. The lower frames show the values of s, in white if $s > 0$ or in black otherwise, whereas the upper frames the values of s^2 in white if $s^2 > .1$ or in black otherwise.

ordered domains in the s^2 pattern, and the specimen is still in the disordered state when observed under an electron microscope. As the ageing is continued, some of the small domains grow up larger, and sometimes coalesce with the neighboring domains, when they are of the same phase, or touch with other domains by APBs, when they are of opposite phases. At this stage the ordered domains change rapidly their sizes and shapes, and some of them grow in magnitude of the degree of order, appearing as ordered regions in the pattern of s^2. After more ageing most of the ordered domains are fully grown, but there still remains some disordered regions among ordered domains. And finally the disordered regions disappear, leaving only the APBs between the domains. These APBs move slowly to make themselves smooth, and small domains keep shrinking and then disappear, to be swallowed by the surrounding large domains of opposite phases. These characteristic features of our simulation is quite consistent with the electron microscopic observations of ordering in Fe_3Al by Matsumura (Photo. 4) and by Park and Allen (1986).

In this respect Park and Allen (1986) made further an interesting experiment. They introduced intersecting APBs in an Fe_3Al specimen by twisting it slightly, and observed the behaviors of APBs *in situ* by an electron microscope at an elevated temperature a little below T_0. They observed that the intersecting APBs are cut and rounded at the intersections. We made a simulation for this process in a mesh of 100 $\times$ 100 by making pairs of intersecting APBs as a starting distribution of $s(\boldsymbol{r}, 0)$, and began the iteration of integration of Eq. (4) in order to pursuit the change of pattern. As is shown in Fig. 3 we found that the APBs with smaller angles always remain to exist, whereas those with larger angles disappear. This tendency is quite in conformity with the actual electron microscopic observation by Park and Allen

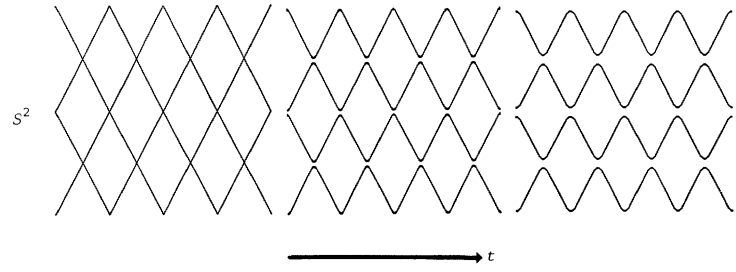

Fig. 3. Change of pattern of a pair of intersecting APBs. In order to demonstrate the effect each frame of the series of simulation in the 100 × 100 mesh is displayed in a 2 × 2 squares. The simulation started from the intersecting APBs in the left side of the figure, and as the iteration of integration of Eq. (4) proceeded to the right, APBs were cut and rounded at the intersection, leaving the APBs of small angles, in conformity with the observation by Park and Allen (1986).

(1986), and looking back also to our own electron micrographs of Fe_3Al, we found some cases which show the result of a similar separation of the intersecting APBs. See the first frame (a) of Photo. 2 (Oki *et al.*, 1977).

We tried also a computer experiment of the shrinkage of a circular domain. From the original equation of motion Eq. (4), it can be shown that a fully grown circular domain of the radius R shrinks approximately at the rate of $dR/dt = -1/R$. In order to test the above rule, we made a large circular domain of the fully ordered state as an initial distribution of $s(\boldsymbol{r}, 0)$ in a mesh of 100 × 100 points, and started the iteration of integration. The result of simulation is shown in Fig. 4, which

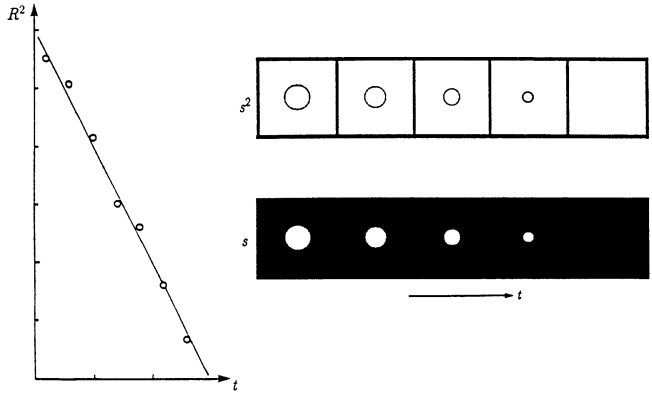

Fig. 4. Simulation of the shrinkage of a circular domain. A large circular domain prepared in the 100 × 100 mesh kept shrinking by ageing and then disappeared. Also shown is the change of the radius R squared vs. t the ageing time.

Table 1. Estimation of the numerical values for some combinations of parameters appearing in Eq. (3), obtained by making comparison of our simulation series with the actual *in situ* observation in Fe-27at%Al. The saturation value of the degree of order was assumed either 1 or 2, whereas the value of the degree of DO_3 order estimated from the composition would be 1.73.

interpretation of observations		Park and Allen, 1986		Allen and Krzanowski, 1985	
temperature	T	745 K		778 K	
degree of order	S_e	1	2	1	2
from correspondence between simulation and electron micrographs	K/B	0.74×10^{-15} m^2	1.47×10^{-15} m^2	0.11×10^{-15} m^2	0.22×10^{-15} m^2
	$L\cdot B$	1.29×10^{-3} s^{-1}	0.32×10^{-3} s^{-1}	11.4×10^{-3} s^{-1}	2.85×10^{-3} s^{-1}
from above	$L\cdot K$	0.9×10^{-18} m^{2}s^{-1}	0.6×10^{-18} m^{2}s^{-1}	1.2×10^{-18} m^{2}s^{-1}	0.6×10^{-18} m^{2}s^{-1}
from shrinkage rate of circular domains	$L\cdot K$	0.6×10^{-18} m^{2}s^{-1}	0.6×10^{-18} m^{2}s^{-1}	1.0×10^{-18} m^{2}s^{-1}	0.8×10^{-18} m^{2}s^{-1}
width of APB	$(K/B)^{1/2}/3$	9.1 nm	12.8 nm	3.5 nm	4.9 nm

includes also the the change of the radius measured on the print-out. As is seen in the figure the result of this simulation is quite satisfactorily interpreted by the $t^{1/2}$-law.

From the comparison between our simulation series, like Fig. 2, and the corresponding *in situ* observations by Park and Allen (1986) and Allen and Krzanowski (1985), we can roughly estimate the numerical values for some combinations of parameters appearing in Eq. (3). Table 1 shows an example of such an analysis, and the mutual consistency of the values of parameters obtained independently, and the reasonable values obtained for the thickness of APBs seem to indicate the adequateness of our interpretation of the evolution of antiphase ordered domain structures in the alloys by using Eq. (3) or (4).

3. Process of Phase Separation Activated by Ordering-the Isotropic Case

We have already seen in Photo. 2 an example of the case, in which the phase separation takes place induced by ordering from B2 to $\alpha + DO_3$ state in the Fe_3Al system. In order to interpret such a process, we suggested a model in which the alloy is regarded as a continuum represented by the two field variables, the local concentration variable $x(\boldsymbol{r}, t)$ of solute atoms, which is conserved, and the local degree of order $s(\boldsymbol{r}, t)$, which is not conserved (Eguchi *et al.*, 1984; Eguchi and Ninomiya, 1988; Shiiyama *et al.*, 1990). The thermodynamical potential of the system $A_{(1-X)/2}B_{(1+X)/2}$ is assumed as

$$F\left[\{x(\boldsymbol{r},t),s(\boldsymbol{r},t)\}\right]=\int\left\{f(x,s)+\left(H(T)/2\right)(\nabla x)^2+\left(K(T)/2\right)(\nabla s)^2\right\}\mathrm{d}^3r, \quad (5)$$

where $x(\boldsymbol{r}, t)$ is the deviation from the average composition X, and the bulk free energy $f(x, s)$ is given by

$$f(x,s)=A(T)x^2-A(T)X_0(T)^2s^2/2+A(T)X_1(T)^2s^4/4+A(T)x^2s^2/2, \quad (6)$$

under the assumption that the order-disorder transformation in this case is of the second order, and that the phase separation cannot take place in the disordered state, but can in the ordered state, provided that the conditions $A > 0$, $0 < X_1 < X_0$ and $X_0^2 + (1-X_1)^2 < 1$ are satisfied. In Fig. 5 the free energy $f(X, S)$ given by (6) is represented as a function of X and S in equi-energy curves, and also the free energy for the equilibrium, $f(X, S_e(X))$ where $\pm S_e(X)$ is the equilibrium degree of order at the temperature under consideration. The spinodal line, which is one-sided here, and the phase boundaries between the mixed phase field and the ordered one or the disordered, in the equilibrium phase diagram, are given by $X_s(T)$ and $X_1(T)$ or $X_2(T)$, respectively, where $X_s = \{(X_0^2 + 2X_1^2)/3\}^{1/2}$ and $X_2 = (X_0^2 + X_1^2)/2X_1$. The phase diagram thus obtained, shown in Fig. 6, resembles the one under consideration in

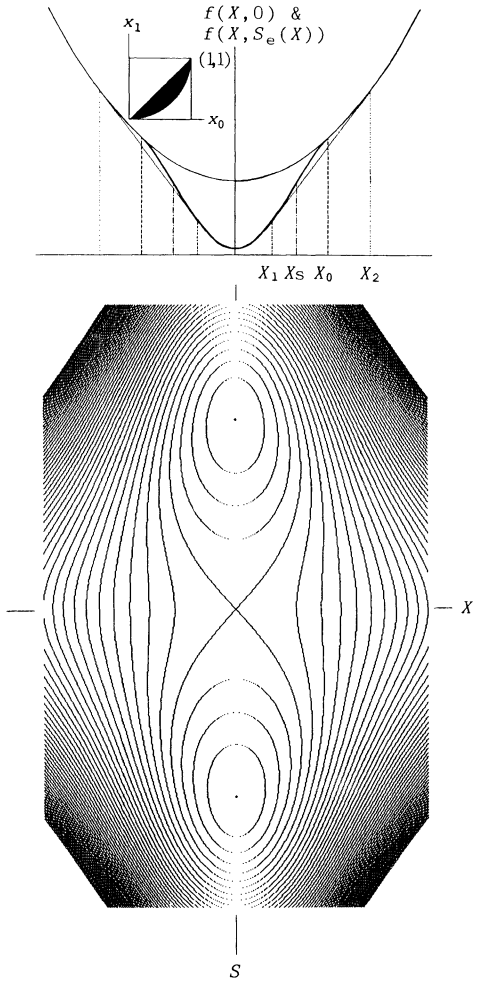

Fig. 5. Free energy $f(X, S)$ of the system, given by (6), as a function of the average composition X and the uniform degree of order S. As can be seen from the equi-energy curves, $f(X, S)$ has a saddle point around $X = S = 0$, which means that the system is stable against a small disturbance in the concentration X, but is unstable against any small one in the degree of order S. Also shown is the free energy for the equilibrium $f(X, S_e(X))$ for the ordered and disordered states. The shaded region in the X_0-X_1 plane is the one in which the conditions for the existence of mixed phase of those states are satisfied.

the Fe_3Al system. Now the equations of motion for the relaxation from the nonequilibrium state are given by $\partial x/\partial t = L(T)\nabla^2(\delta F/\delta x)$ and $\partial s/\partial t = -M(T)(\delta F/\delta s)$ with $L(T)$ and $M(T)$ as the positive reaction rates. These equations are rewritten as

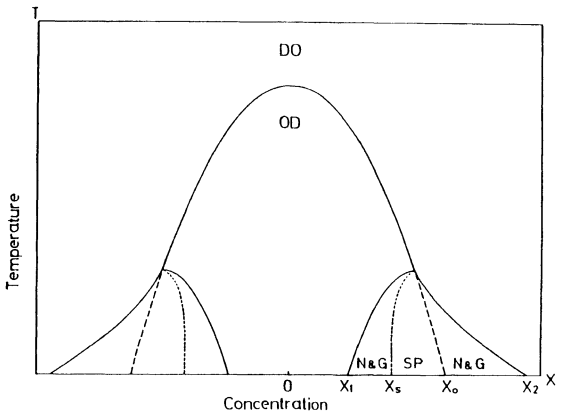

Fig. 6. An example of the equilibrium phase diagram obtained from the free energy $f(X, S)$ under the conditions given in the text. Note the existence of the mixed phase of the ordered and disordered states. See the curves for the equilibrium free energy $f(X, S_e(X))$ in Fig. 5.

follows, after a suitable scaling into a dimensionless space-time world (Eguchi and Ninomiya, 1988):

$$\partial x / \partial t = -\nabla^4 x + 2\nabla^2 x + \nabla^2\left(xs^2\right)$$
$$\text{and} \quad \partial s / \partial t = \alpha s\left(X_0^2 - x^2 - X_1^2 s^2\right) + \beta\nabla^2 s, \tag{7}$$

where α and β are certain parameters depending upon the ageing temperature. A series of the two-dimensional simulation in a mesh of 200 × 200 points are reproduced in Fig. 7, where the patterns of $s(\boldsymbol{r}, t)$, $s(\boldsymbol{r}, t)^2$ and $x(\boldsymbol{r}, t)$ are given in time sequence of ageing. Here again we started from the disordered state in a uniform composition, with small noises in $x(r, 0)$ and $s(r, 0)$ around zero level, and the iteration of integration by every short time interval was carried out.

As the iteration proceeds the noises in the x-field once almost disappear, because the system is stable against any small changes in the composition (see Fig. 5), but the changes in the s-field is pronounced, and through the coupling between the two fields, the x-field is activated in a kind of a resonant way to the s-field (Eguchi *et al.*, 1984). The evolution of the patterns of s^2 in our simulation has a remarkable resemblance with our observation of the process of phase separation induced by ordering, shown in the dark field images of Fe_3Al taken with an electron microscope by the use of DO_3 superstructure reflection (Oki *et al.*, 1974, 1977). Thus, we are confident that the process of ordering and phase separation occurring in Fe_3Al was consistently accounted for by our model with the thermodynamical potential (5) and

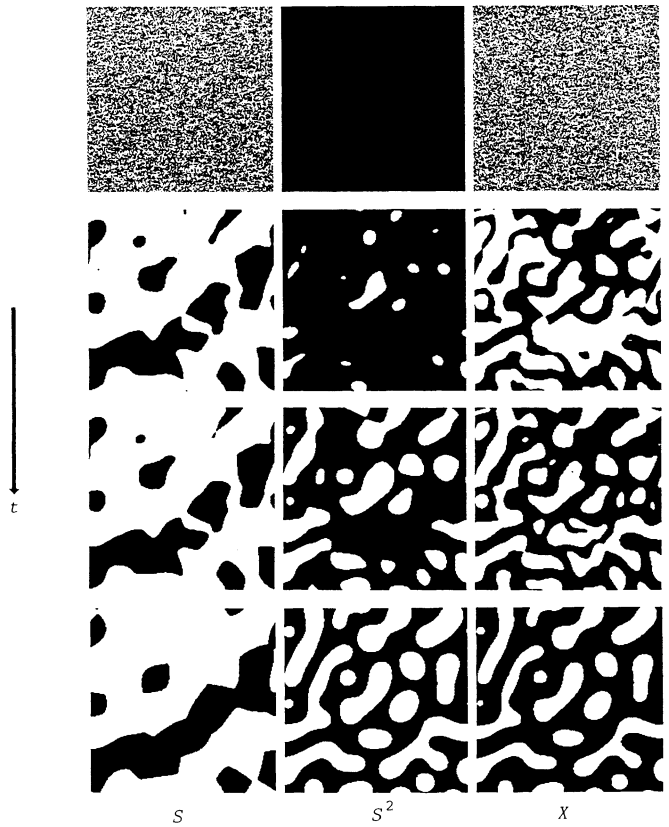

Fig. 7. A set of examples of two-dimensional simulation for the process of isotropic phase separation induced by ordering, described by Eqs. (7). In the figure the values of $x(\boldsymbol{r}, t)$ are expressed in white if $x < 0$, or in black otherwise, whereas those of $s(\boldsymbol{r}, t)$ and $s(\boldsymbol{r}, t)^2$ in the same way as before. The patterns of s^2 correspond to the dark field images in electron micrography.

(6), and the equations of motions (7) derived from it.

4. Anisotropic Phase Separation Induced by Ordering

As mentioned in the introduction, Fe-Si alloy behaves in a similar way as Fe-Al system, but the main difference between the two lies in the fact that although the antiphase ordered domain structure in Fe-Al is apparently isotropic without any preferential direction for the APBs and the boundaries between ordered and disordered phases, but that in the case of Fe-Si system the domain structure is highly anisotropic. Matsumura, Oyama and Oki (1989) carefully investigated the process

in Fe-Si under an electron microscope, and found that the evolution of the patterns of ordered domains seemed isotropic up to the intermediate stage of ageing, but that in the later stage they became anisotropic with almost rectangular Si-rich ordered precipitates in the disordered matrix with less Si. The process they observed is clearly recognized in Photo. 6, which comprises a series of electron micrographs of dark field images, taken with the same sample but with the various ageing times.

In order to interpret such a process theoretically, and to make a simple simulation using equations of motions for $x(\boldsymbol{r}, t)$ and $s(\boldsymbol{r}, t)$ with a result of anisotropic phase separation, a straightforward way would be to consider the microelasticity, as was done by Cahn (1962), due to the lattice distortion in the regions of varying composition, which arises from the difference of lattice parameters of the component metals. We did not, however, follow this elaborate work, but took a phenomenological approach to generalize the equation of motion for the phase separation to include the anisotropy. In order to illustrate our method, we consider first a simple case of spinodal decomposition in a disordered alloy with a nonlinear effect, which is described by the thermodynamical potential:

$$F\left[\{x(\boldsymbol{r},t)\}\right] = \int \left\{ f(x) + \left(H(T)/2\right)(\nabla x)^2 \right\} \mathrm{d}^3 r,$$

$$\text{with} \quad f(x) = A(T) - B(T)X_0^2 x^2/2 + B(T)x^4/4, \tag{8}$$

which leads to the equation of motion:

$$\partial x/\partial t = -L(T)H(T)\nabla^4 x - L(T)B(T)\left(X_0^2 - 3x^2\right)\nabla^2 x + 6L(T)B(T)x(\nabla x)^2, \tag{9}$$

where $A(T)$ and $B(T)$ are certain positive parameters, whereas $\pm X_0(T)$ are the phase boundaries and $\pm X_s(T) = \pm X_0(T)/\sqrt{3}$ are the spinodals. Equation (9) is essentially Cahn's equation for spinodal decomposition (Cahn and Hilliard, 1958, 1959; Cahn, 1961), but for the last nonlinear term which prevents the numerical solutions from overflow. When the decomposition has some preferential directions, then the isotropic equation (9) has to be generalized, so that the whole equation is invariant under any rotation, but that the coefficient of the derivatives must be slightly modified by regarding them as tensors.

Thus $LH\nabla^4 x$ must be replaced by $\Sigma(LH)_{\alpha\beta\gamma\delta}\partial^4 x/\partial r_\alpha \partial r_\beta \partial r_\gamma \partial r_\delta$, $LB\nabla^2 x$ by $\Sigma(LB)_{\alpha\beta}\partial^2 x/\partial r_\alpha \partial r_\beta$, and $LB(\nabla x)^2$ by $\Sigma(LB)_{\alpha\beta}(\partial x/\partial r_\alpha)(\partial x/\partial r_\beta)$. If the sample under investigation is of a cubic lattice, as is the case of Fe-Al and Fe-Si systems, then the cubic symmetry reduces the rank of tensors concerned or the number of their independent components. Thus the symmetric tensor of the second rank becomes a scalar, and the tensor of the fourth rank with a complete symmetry reduces its number of independent components into two, say Γ_{11} and Γ_{12} in the conventional

notation, and finally the equation of motion (9) is modified as, after a suitable scaling:

$$\partial u / \partial \tau = -\nabla^4 u + 2\gamma \nabla'^4 u - \left(1 - u^2\right)\nabla^2 u + 2u(\nabla u)^2, \tag{10}$$

where $u(\rho, \tau)$ is a variable proportional to $x(\boldsymbol{r}, t)$, and γ is a new parameter representing the anisotropy, or $\gamma = \Gamma_{12}/\Gamma_{11}$, with $\gamma = 0$ a special case for the isotropy. The new symbol ∇'^4 represents $\nabla'^4 = \partial^4/\partial\eta^2\partial\zeta^2 + \partial^4/\partial\zeta^2\partial\xi^2 + \partial^4/\partial\xi^2\partial\eta^2$. Here we have changed our space-time world $(\boldsymbol{r}, t)$ into a new dimensionless one (ρ, τ), where the space coordinates are written as ξ, η and ζ. In order to see how the value of γ affects the patterns of phase separation, we demonstrated in Fig. 8 the evolution of the patterns of $u(\rho, \tau)$ for the three cases of $\gamma = +1, 0, -2$. In the figure, the readers will

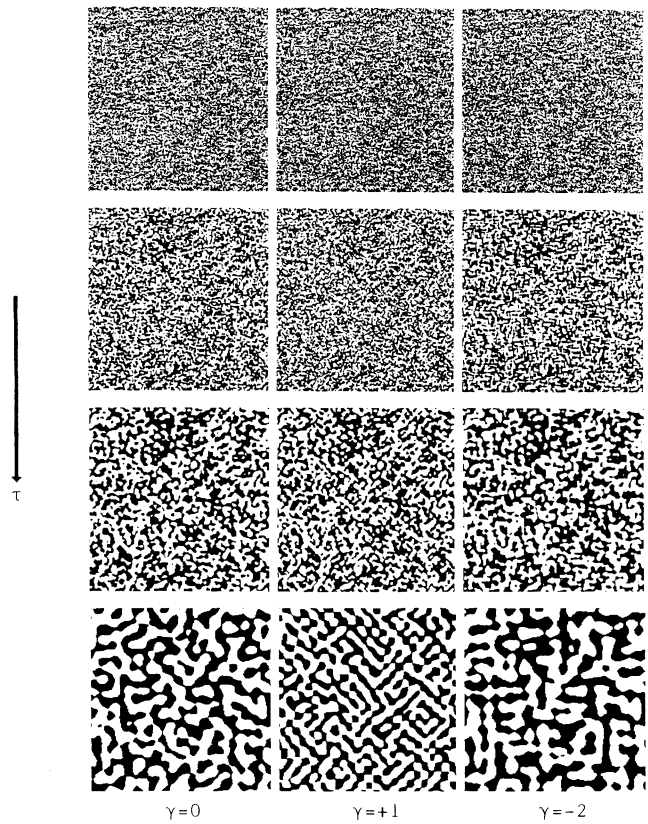

Fig. 8. Examples of two-dimensional simulations for the process of anisotropic spinodal phase separation, described by Eq. (10), for $\gamma = 0$, +1 and –2.

see that the patterns started from the same fine and small distribution of the deviation in the solute concentration, and little hint of anisotropy could be recognized, in any of the three cases, up to the intermediate stage of ageing, but that in the later stage, as the deviation became larger, the directional preferences became distinct in the cases of nonvanishing γ, and in the last stage the patterns of the deviation are predominant in the <111> direction in the case of $\gamma = +1$ or in the <100> in the case of $\gamma = -2$. In the case of $\gamma = 0$, on the contrary, no trace of preferential directions is discerned, as was expected by the theory. In the actual spinodal decomposition in the alloys of cubic lattice, the patterns observed under electron microscopes are well known to be either one of these three cases.

Now, in order to simulate the phase separation in Fe-Si system observed by Matsumura, Oyama and Oki (1989), which we have already seen in Photo. 4, we have made a generalization to the coupled equations of motion Eqs. (7), similar to the one we made in Eq. (9) to obtain (10). Thus the new set of equations are:

$$\partial x / \partial t = -\nabla^4 x + 2\gamma\nabla'^4 x + 2\nabla^2 x + \nabla^2\left(xs^2\right),$$

$$\text{and} \quad \partial s / \partial t = \alpha s\left(X_0^2 - x^2 - X_1^2 s^2\right) + \beta\nabla^2 s. \tag{11}$$

The simulation developed in Section 3 was the special case of isotropy, $\gamma = 0$. To simulate the case of Fe-Si system, we chose tentatively the case of $\gamma = -2$, and tried a various set of values for other parameters. In Fig. 9 the result of one of our simulation patterns is shown, which we consider is most likely to be compared with the observed one. In the figure it is seen in the pattern of s^2, which corresponds to the dark field images of electron micrography, that the evolution of ordered domains is expected isotropic up to a certain intermediate stage of ageing, but that, as the change in s is reflected in the change of x, the pattern of s^2 becomes gradually anisotropic, and finally the rectangular precipitates are formed in the pattern of x. In this last stage the pattern of s^2 is almost similar to the one of x, but a small difference is noticed between the two in the sense that in the s^2 pattern large ordered domains are rectangular, but the small ones are circular, in contrast to the x pattern where all precipitates are rectangular. In this connection readers are to be reminded that the patterns of s^2 were made to represent the regions in white if $s^2 > .1$. When this criterion is raised a little, for example $s^2 > .15$, then we obtain the pattern shown in Fig. 10, which is almost identical with that of x. This shows, on one hand, that the pattern of compositional variation can be guessed properly by the pattern of ordered domains only after an enough time has elapsed for ageing, and that the absolute magnitude of the degree of order should be sufficiently high for that purpose, on the other. Up to the intermediate stage of ageing the patterns of $x(\boldsymbol{r}, t)$ and $s(\boldsymbol{r}, t)$ are largely different from each other.

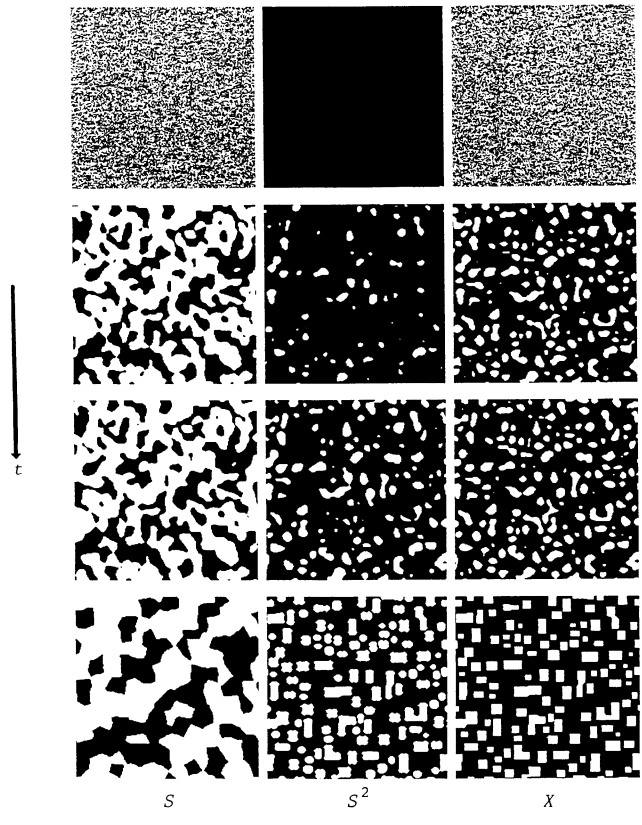

Fig. 9. A set of examples of two-dimensional simulation for the process of anisotropic phase separation induced by ordering, described by Eqs. (11). The anisotropy parameter γ is assumed to be -2. The values of $s(\boldsymbol{r}, t)^2$ are expressed in white if $s^2 > .1$ in the same way as before.

Fig. 10. The last frames of the simulation patterns of Fig. 9, but the values of $s(\boldsymbol{r}, t)^2$ are expressed in white if $s^2 > .15$. See the similarity of the pattern of $s(\boldsymbol{r}, t)^2$ to that of $x(\boldsymbol{r}, t)$, which is expressed in white if $x < 0$.

5. Conclusion

In the development of the theory and the simulations described above, the alloys were assumed to be a continuum, whose local state of phases is represented by the local composition, which is conserved, and the local degree of order, which is not conserved. The equations of motion to describe the local dynamics of phase transition were derived by the so-called TDGL (time dependent Ginzburg-Landau) method, from the thermodynamical potentials appropriately assumed to include the physical essence of the processes in compact forms, or the equations were generalized under the consideration of transformation characters and symmetry. In the three different cases of the simulation, our results were quite consistent with the actual observations of the evolution of patterns of ordered domains, by the method of dark field images in the electron microscopy, and showed the reasonableness of our interpretation, that in some alloys such as Fe-Al or Fe-Si the phase separation is activated only by ordering (Eguchi *et al.*, 1984). The problems are left, however, untouched for the future tasks to investigate the patterns in more complicated ordering processes, especially those in the first order transitions or in the cases in which more than one degrees of order are involved. There is also a standing problem to find a linkage between the atomic discrete model and the continuum approximation. The phenomenological generalization of the equation of motion developed in the last section has to be derived directly from the microelasticity approach. In this respect an elaborate work by Onuki (1990) might be attractive. We should like, however, to stress the powerfulness of the TDGL method within a continuum model to interpret the physical background of phase transitions.

Acknowledgements

Thanks are due to Professor Allen at MIT for valuable discussions on his work in comparison with our simulations, and to Drs. Tomokiyo and Matsumura of Kyushu University for their kindness to permit us to use their fine electron micrographs.

REFERENCES

Allen, S. M. and Krzanowski, J. E. (1985), Proc. Intern. Conf. Solute-Defect Interaction: Theory and Experiment, Ontario, CANADA, 400.

Cahn, J. W. (1961), Acta Metall., **9**, 795.

Cahn, J. W. and Hilliard, J. E. (1958), J. Chem. Phys., **28**, 258.

Cahn, J. W. and Hilliard, J. E. (1959), J. Chem. Phys., **31**, 688.

Cahn, J. W. (1962), Acta Metall., **10**, 179.

Eguchi, T., Oki, K., and Matsumura, S. (1984), Mat. Res. Soc. Symp. Proc., **21**, 589.

Eguchi, T. and Ninomiya, H. (1988), "Dynamics of Ordering Processes in Condensed Matter", edited by Komura, S. and Furukawa, H., 151 pp., Plenum Pub. Co., New York and London.

Krzanowski, J. E. and Allen, S. M.(1986), Acta Metall., **34**, 1035 and 1045.

Matsumura, S., Oyama, H., and Oki, K. (1989), Mat. Trans. JIM, **30**, 695.

Matsumura, S. (1990), private communication.
Ninomiya, H., Kanemoto, H., and Eguchi, T. (1990), Phase Transitions B, **28**, 125.
Oki, K., Sagane, H., and Eguchi, T. (1974), Japan Journ. Appl. Phys., **13**, 753.
Oki, K., Sagane, H., and Eguchi, T. (1977), Journ. de Phys., **C-7**, 414.
Oki, K., Matsumura, S., and Eguchi, T. (1987), Phase Transitions B, **10**, 257.
Onuki, A. (1990), Proc. Intern. Workshop on Computational Materials Science, Tsukuba, Japan, 227, published by Nat. Res. Inst. Metals.
Park, W. and Allen, S. M. (1986), Mat. Res. Soc. Symp. Proc., **62**, 303.
Shiiyama, K., Kanemoto, H., Ninomiya, H., and Eguchi, T. (1990), Proc. Intern. Workshop on Computational Materials Science, Tsukuba, Japan, 103, Published by Nat. Res. Inst. Metals.
Tomokiyo, Y. (1989), private communication.